

Published in final edited form as:

Trends Mol Med. 2010 December ; 16(12): 574–583. doi:10.1016/j.molmed.2010.08.006.

Near-infrared fluorescent nanoprobe for cancer molecular imaging: status and challenges

Xiaoxiao He^{†,1,2}, Jinhao Gao^{†,1,3}, Sanjiv Sam Gambhir^{1,4}, and Zhen Cheng^{*,1}

¹Molecular Imaging Program at Stanford (MIPS), Department of Radiology, Bio-X Program and Stanford Cancer Center, Stanford University School of Medicine, Stanford, California 94305, USA

²State Key Laboratory of Chemo/Biosensing and Chemometrics, Institute of Biology, Hunan University, Changsha 410082, P.R. China

³Department of Chemical Biology, College of Chemistry and Chemical Engineering, Xiamen University, Xiamen 361005, P.R. China

⁴Departments of Radiology and Bioengineering, Stanford University, Stanford, California 94305, USA

Abstract

Near-infrared fluorescence (NIRF) imaging promises to improve cancer imaging and management; advances in nanomaterials allow scientists to combine new nanoparticles with NIRF imaging techniques, thereby fulfilling this promise. Here, we present a synopsis of current developments in NIRF nanoprobe, their use in imaging small living subjects, their pharmacokinetics and toxicity and finally their integration into multimodal imaging strategies. We also discuss challenges impeding the clinical translation of NIRF nanoprobe for molecular imaging of cancer. Whereas utilization of most NIRF nanoprobe remains at a proof-of-principle stage, optimizing the impact of nanomedicine in cancer patient diagnosis and management will likely be realized through persistent interdisciplinary amalgamation of diverse research fields.

Keywords

NIRF nanoprobe; molecular imaging; clinical translation; QDs; nanotubes

Molecular imaging and nanotechnology

Cancer molecular imaging is an evolving field in which diverse optical tools and strategies are used for early detection and management of tumors. This field arose from the merger of several pre-existing disciplines such as modern cancer molecular biology, chemistry and imaging technologies. Consequently, cancer molecular imaging has created unique opportunities to study and noninvasively monitor tumor genesis, development and

© 2010 Elsevier Ltd. All rights reserved.

* Corresponding Author: Zhen Cheng, PhD, Assistant Professor, Molecular Imaging Program at Stanford, Department of Radiology, 1201 Welch Road, Lucas Center, P020A, Stanford University, Stanford, CA, 94305-5484, Phone: 650-723-7866, Fax: 650-736-7925, zcheng@stanford.edu.

[†]equal contribution

Publisher's Disclaimer: This is a PDF file of an unedited manuscript that has been accepted for publication. As a service to our customers we are providing this early version of the manuscript. The manuscript will undergo copyediting, typesetting, and review of the resulting proof before it is published in its final citable form. Please note that during the production process errors may be discovered which could affect the content, and all legal disclaimers that apply to the journal pertain.

metastasis *in vivo* [1,2]. It is expected to provide more comprehensive anatomical, physiological and functional information of diseases in a clinical setting. Molecular imaging techniques could be powerful tools in early cancer detection, drug discovery and development as well as monitoring response to treatment [3–5]. There are a variety of well-established imaging modalities, such as positron-emission tomography (PET) [3,6], single photon emission computed tomography (SPECT) [7], magnetic resonance imaging (MRI) [8–10] and optical fluorescence imaging [11–13], that effectively image specific tumor associated molecular targets.

Here, we describe the development of near-infrared fluorescence (NIRF) nanoprobes for cancer molecular imaging. Because NIRF imaging (650–900 nm) displays properties of low absorption and relatively low autofluorescence, it offers several advantages over other modalities for imaging living organisms. In addition, NIRF imaging has potentially high spatial resolution, high sensitivity and low risk to the living subject because it utilizes nonionizing radiation. Moreover, it is cost efficient in terms of preparation of molecular probes and the detection hardware is relatively simple to operate.

The integration of nanotechnology with molecular biology and medicine has resulted in active developments of an emerging research area, namely nanobiotechnology. This research offers exciting and abundant opportunities for discovering new materials and tools for biomedicine. Recent advancements in functional nanomaterials offer to improve detection sensitivity and specificity in molecular imaging [14]. Functional nanomaterial-based molecular probes, namely nanoprobes, could target tumors either through the enhanced permeability and retention (EPR) effect of the tumor microvasculature or by the specific binding with tumor-associated biomarkers such as tumor cell receptors, tumor extracellular matrix and enzymes. A variety of nanoprobes have been prepared, evaluated and applied in various imaging modalities including: fluorescence, MRI, radionuclide, Raman and photoacoustic imaging. Examples of probes include gold (Au) nanoparticles (nano-shells, nano-rods and nano-cages) or single wall carbon nanotubes (SWNT) for photoacoustic imaging based on heating effects [15,16]; magnetic iron oxide nanoparticles for MRI [17]; and fluorescent nanoparticles for *in vivo* fluorescence imaging [18]. Nanoparticle-based NIRF probes can overcome several limitations of conventional NIR organic dyes, such as poor hydrophilicity and photostability, low quantum yield and detection sensitivity, insufficient stability in biological systems and weak multiplexing capability.

In this short review, we focus on the latest progress in NIRF nanoprobes for cancer molecular imaging. More specifically, we summarize the development of different types of NIRF nanoprobes, their use for molecular imaging in living subjects, the potential toxicity of NIRF nanoprobes and the combination of NIRF-nanoprobe imaging with several other imaging techniques. We also discuss future perspectives of the NIRF nanoprobes for cancer molecular imaging.

Development of NIRF nanoprobes

Although the number of NIRF nanoprobes is rapidly increasing, most of them can be classified into two major categories: down conversion (DCN) and up conversion (UCN) NIRF nanoprobes. DCN nanoprobes produce low energy fluorescence when they are excited by high energy light. The well-established DCN NIRF nanoprobes include NIRF dye-containing nanoparticles, quantum dots (QDs), SWNTs and metal nanoclusters (Figure 1). By contrast, UCN nanoprobes, which are emerging as a new class of fluorescent nanoparticles and biolabels [19], can convert excitation light with longer wavelength (low energy) to shorter wavelength fluorescence (high energy). In this section, we focus on well-

established NIRF nanoprobes: NIRF dye-containing nanoparticles, NIR fluorescent QDs, SWNTs and Au nanoclusters.

NIRF dye-containing nanoprobes

NIRF dye-containing nanoprobes are organic or inorganic matrix-based nanomaterials that either incorporate NIRF dyes inside the matrix (dye-doped) or attach the reporting molecules to the nanoparticles surface [18]. The matrix should be optically transparent to allow excitation and emission light to pass efficiently. Inorganic matrices for dye encapsulation encompass mainly silica and calcium phosphate nanoparticles [20,21]. Silica matrix is attractive for *in vivo* imaging because its hydrophilic nature can reduce nonspecific binding and aggregation; it is also chemically inert, transparent and easily modified through chemistry. Organic nanocarriers, such as liposomes, micelles and dendrimers, have been used for drug-delivery research for years. Organic systems that encapsulate NIRF dyes for cancer molecular imaging have also been reported [22–24], for example, the water-soluble polymeric nanoparticles were used as carriers of NIRF dyes for tumor imaging [25,26].

Compared to the bare NIR fluorochromes, there are several distinctive features in the NIRF dye-containing nanoprobes. Firstly, the polymer or inorganic matrix encapsulation provides a protective layer around NIRF molecules that reduces their exposure to oxygen both in air and in aqueous media. Encapsulation also prevents direct interaction between NIRF dyes and host tissue. As a result, photostability and biocompatibility of NIRF dye-containing nanoprobes *in vivo* increases substantially in comparison to the bare dyes. Secondly, by using well-established bioconjugation chemistry, the surface of dye-doped nanoparticles can be easily modified with a variety of biomolecules, such as proteins, peptides, antibodies or oligonucleotides. These biomolecules affect the pharmacokinetics of the nanoparticle and make specific molecular targeting possible. Thirdly, the NIRF signal can be enhanced because of the high payload of dye molecules per nanoparticle, which results in much higher sensitivity compared to free fluorochromes [25]. For example, about 600 indocyanine green (ICG) molecules can be doped into each calcium phosphate nanoparticle (CPNP), exhibiting significantly greater intensity at the maximum emission wavelength relative to the free constituent fluorophore [20].

NIR fluorescent and self-illuminating QDs

QDs are a special class of materials known as semiconductors. Because of their unique optical properties, such as size-tunable photoluminescent emission, narrow and symmetric emission spectra, broad absorption spectra and photostability, the use of QDs as fluorescent biotags for cell staining and disease detection is one of the most attractive applications in nanomedicine research [27–29]. The synthesis, surface modification, characterization and application of QDs in the visible spectrum have been reviewed previously [30–32]. As a new class of fluorescent probes, QDs could overcome the limitations of organic dyes and they have high potential for cancer molecular imaging. Still, the main barriers preventing the *in vivo* application of QDs excited by an external illumination source in the visible spectrum are autofluorescence and light scattering within tissues. Therefore, increasing attention has been paid to NIRF-emitting QDs, because with NIRF-QDs, tissue autofluorescence is considerably reduced and the tissue penetration of the excitation light is significantly enhanced [33]. Because of high interest and demand for NIRF-emitting QDs, the development and the synthesis of NIR QDs including cadmium (Cd) and noncadmium based QDs have progressed rapidly. Examples include CdTe (Cadmium telluride)/ZnS (Zinc sulfide) [34], CdTe/CdSe (Cadmium selenide) [35], InAs (Indium arsenide)/InP (Indium phosphide)/ZnSe [36], CuInSe₂ (Copper indium diselenide) [37], and Cu-doped InP/ZnSe [38] QDs.

However, Cd-based QDs showed cytotoxicity *in vitro* under extreme conditions [39,40]. To avoid such toxicity problems, the Cd metal can be replaced by other more benign elements. For example, CuInS₂/ZnS core/shell QDs do not contain any Class A elements [e.g. Cd, Pb (lead) and Hg (mercury)] [41] and have potential as biocompatible probes for biomedical applications. Recently, novel optical probes such as carbon dots and silicon nanoparticles have aroused interest because of their low toxicity [42–44].

In addition to the tunability of emission in the NIR region, the amount of incident excitation light that reaches fluorescent objects *in vivo* can be limited. Bioluminescence resonance energy transfer (BRET), which converts chemical energy from a chemical reaction catalyzed by a donor enzyme rather than the absorption of excitation photons into light energy, has been used to circumvent this issue [45,46]. So and colleagues reported self-illuminating NIR QDs by BRET without the need of external illumination [47–49]. In these studies, QDs, the acceptor in a BRET system, were covalently conjugated to the donor, Renilla luciferase (Luc8) [50]. Upon interaction with its substrate coelenterazine, the Luc8 protein emits blue light with a peak at 480 nm. This light excites QD-Luc8 conjugates to produce NIR light (Figure 2a). The key advantage of using bioluminescence is the elimination of autofluorescence as no external light excitation is needed (Figure 2a, b). This “self-illuminating” feature could allow molecular imaging of cancer in deeper tissue. Because no excitation light is needed, light scattering from the tissue and the toxicity to the tissue from excitation photons are also avoided. However, substrate must still be delivered for BRET. In another study, radiation produced light with broad continuous wavelengths (ultraviolet-visible to NIR), which can excite fluorescent materials such as QDs (Figure 2c). This provides an alternative strategy for the design of self-illuminating nanoprobes. By marrying this technique with the intrinsic property of QDs (e.g. the capacity of simultaneous excitation of multiple fluorescent colors), multiplexing *in vivo* imaging with radionuclides (e.g. ¹³¹Iodine) can become a reality (Figure 2d). Radiation-luminescence excited nanoprobes might have advantages in multiplex fluorescence imaging as well as multimodality imaging [51].

Carbon nanotubes

Carbon nanotubes (CNTs) can be broadly classified as SWNTs and multiwalled nanotubes (MWNTs). Both categories have attracted interest for their unique electronic, metallic and structural characteristics. Traditionally, most research on CNTs has focused on their mechanical, thermal and electronic properties and their potential application in electronic devices. Since 2002 and the discovery of fluorescent semiconducting CNTs, research into CNTs for their optical properties and their application to bioimaging have accelerated [52–55].

SWNTs can be viewed of as a rolled graphene (a single plane of graphite sheet) and are classified by a vector connecting the two points that meet upon rolling (Figure 1). The rolled single tube is approximately 1 nm in diameter and several hundred nanometers to 100! m in length. Depending on how a nanotube is wrapped up from a single plane of graphene, it can be semiconducting or metallic. SWNTs are promising NIRF nanomaterials for molecular imaging because they have the following features. First, the emission of SWNT-based NIRF probes are mostly in the infrared-A region (IR-A, 1–1.4 μm), making them ideal for *in vivo* imaging because of low biological autofluorescence. Second, there is a large Stoke's shift between the excitation and emission bands of SWNTs, making it possible to excite the nanoparticles in the NIR window thereby reducing further autofluorescence and scattering. Third, SWNTs possess high surface area and can load large amounts of targeting ligands or drugs. Last, SWNTs are highly photostable, unlike conventional fluorophores, which allows them to serve as long-term NIRF tracking probes *in vivo* [54]. However, the fluorescence of SWNTs can be quenched when they are aggregated in bundles. Biocompatible SWNTs with

high quantum yield are elusive, which might limit their use in cancer fluorescence imaging. In the future, chemical modification will play a key role in the fabrication of high performance of SWNTs for optical imaging.

Au nanoclusters

Nanometer-sized Au particles are one of the most important classes of metal nanoparticles and have been used widely to stain cells and tissue samples for electron microscopy. Au nanoparticles do not emit fluorescence but effectively scatter light, exhibiting a range of intense colors in the visible and NIR spectra. Au nanoparticle-based bioanalytic method is a promising technique for detecting a wide range of biological macromolecules because it offers distinct Raman signatures (see Glossary) and easy surface functionalization. Au-based nanomaterials, such as nanoparticles, nanoshells and nanorods, have also been used as contrast agents for imaging cancer *in vivo* by taking advantage of their surface plasmon (SP) bands in the NIR region [56–59]. Interestingly, emission from small Au nanoclusters with sizes below 2 nm has gained significant attention. All Au nanoclusters are a collection of a small number of Au atoms (Figure 1), which have sizes comparable to the Fermi wavelength (see Glossary), resulting in molecule-like behavior including discrete electronic states and size-dependent fluorescence [60]. Au nanoclusters are attractive for bioimaging applications because of their potential for low toxicity and their ultrafine size. Au nanoclusters with emissions from blue to red have been reported by using poly(amidoamine) dendrimer (PAMAM), mercaptoundecanoic acid (MUA) and lipoic acid (DHLLA) as nanoparticle templates or ligands [61–63]. Recently, advances in green chemistry with environmentally friendly methods have made it possible to prepare NIR Au nanoclusters using bovine serum albumin (BSA) as a template at physiological temperature [64]. The emergence of NIRF Au nanoclusters that possess advantages of both small size and brightness opens a new path toward *in vivo* imaging applications.

NIRF nanoprobe for cancer molecular imaging

One of the major concerns for imaging with NIRF nanoparticles in living subjects is specificity. Three approaches have been applied for tumor targeting of NIRF nanoparticles: (i) the well-known EPR effect, (ii) molecular targeting via specific antigens or overexpressed receptors on the surface of cancer cells, and (iii) the chemical activation of the nanoprobe in specific tumor microenvironments (e.g. enzymatic cleavage or oxidation).

Passive targeting of NIRF nanoprobe

Compared with normal cells, cancer cells tend to proliferate rapidly and secrete factors that promote the formation of tumor-associated neovasculature from the existing vasculature. This produces the well-known EPR effect; the tumor-associated neovasculature has large interendothelial junctions, an imperfect basement membrane, an inefficient lymphatic system and large numbers of transendothelial channels. Furthermore, tumor tissues tend to have poor lymphatic drainage. Selective targeting of tumor tissue with nanoparticles can be achieved by taking advantage of the EPR effect of the tumor microvasculature and the poor lymphatic drainage of tumors [65]. Nanoparticles ranging from 10–100 nm might escape renal filtration and accumulate in tumors after prolonged circulation [66]. The level of nanoparticle accumulation in tumors depends both on the properties of the nanoparticles and the type of the tumor. Variables include the size, surface modification and the half-life of the nanoparticles in circulation, as well as the leakiness of vascular pore, the degree of tumor vascularization and the degree of angiogenesis in the tumor. NIRF dye-containing nanoparticles have much longer circulation times than free NIRF dyes, which by consequence encourages the accumulation in tumors through the EPR effect. This accumulation enhances the imaging signal, which comes from both the selective trapping of

the nanoparticles as well as an amplification and protection effect owing to their encapsulation. Altinoglu and colleagues [20] used biodegradable CPNP encapsulated with the NIR-emitting fluorophore ICG as a new fluorescent nanoprobe for sensitive diagnostic imaging. The CPNP with an average size of 16 nm in diameter prolonged circulation time *in vivo* with high passive tumor accumulation of the nanoparticles in solid xenograft breast adenocarcinoma tumors within 24 h of systemic tail vein injection [20].

For the passive delivery of QDs, the efficiency of targeting relies on the inherent physicochemical properties of the QDs (e.g. particles size, charge and surface properties). One critical issue for applications of QDs in living subjects is the hydrodynamic diameter (HD) of nanoparticles. QDs with large diameters (>20 nm) suffer from extremely high uptake in both RES and the mononuclear phagocytic system (MPS), which reduces their efficiency and sensitivity. Ultrasmall water-soluble QDs (<10 nm) have attracted increasing attention because their unique properties, rapid renal clearance [43,44,67,68], low RES uptake and the possibility of EPR effect, are advantageous for *in vivo* applications. Recently, Gao and colleagues reported high tumor uptake of ultrasmall NIR noncadmium QDs owing to the EPR effect [69].

Because of the small size of vessels and poor access, *in vivo* visualization of the lymphatic function is relatively difficult. Kim and colleagues reported the utility of NIR QDs (CdTe/CdSe) for sentinel lymph node imaging in both mouse and porcine models. QDs translocate to sentinel lymph nodes, likely from the combination of passive flow in lymphatic vessels and the active migration of dendritic cells that engulfed the nanoparticles [35]. Subsequently, Hama and colleagues showed simultaneous *in vivo* two-color wavelength-resolved spectral fluorescence lymphangiography using two NIR CdTe-based QDs with different emission spectra (705 and 800 nm). Two-color spectral fluorescence lymphangiography can provide insight into drainage from different lymphatic basins that can detect sentinel lymph nodes of the breast cancer and prevent complications such as lymphedema of the arm [70].

Although SWNTs are relatively long (0.5–2 μm), *in vivo* fluorescence imaging by semiconducting SWNTs is still possible owing to their flexible structure. Welsher and colleagues developed bright fluorescent SWNTs by sonicating SWNTs with sodium cholate, followed by surfactant exchange to form phospholipid–polyethylene glycol (PEG) coated nanotubes. Using this type of SWNT, high-resolution intravital images of tumor vessels below the skin of mice were obtained [71]; these SWNTs might have applications in image-guided surgery.

Targeted molecular imaging of NIRF nanoprobe

In contrast to gross structural imaging, the advantage of molecular imaging is the potential to reveal differences between cancerous and normal tissues at the molecular level. To realize this potential, NIRF nanoprobe need to be modified with biomolecules that facilitate binding only in the targeted locations. A variety of targeting groups have been developed for the modification and functionalization of NIRF nanoprobe, such as small molecules, peptides, proteins, aptamers, engineered antibodies and antibody-based ligands [12,13,29]. Targeted NIRF nanoprobe might significantly improve the efficiency (specificity and selectivity) of delivery to the tissue of interest.

Using small animals as models, Gao and colleagues first described *in vivo* cancer targeting with QD-antibody conjugates [72]. Subsequently, numerous publications have reported targeted molecular imaging of cancer via QDs with peptides and proteins as the main targeting biomolecules. *In vivo* targeted imaging of tumor vasculature was achieved using peptide-conjugated NIR QDs [73–75] through surface modification of NIR QDs with

arginine-glycine-aspartic acid (RGD) peptides to produce constructs known as QD-RGDs. The QD-RGDs showed specific and strong binding to integrin $\alpha_v\beta_3$ -positive vasculature to human xenografts implanted into nude mice. However, the relatively large size of the QD-RGD (~20 nm in HD) prevented efficient extravasation, thus QD-RGD mainly targeted the tumor vasculature instead of the tumor cells. The *in vivo* targeting behavior of QD-RGD has also been demonstrated in tumor vessels by intravital imaging of QD800-RGD in real time [76]. As shown in Figure 3, QD800-RGD does not extravasate in an SKOV-3 mouse ear tumor model; QD800-RGDs specifically bind the tumor neovasculature as aggregates, but no binding occurs for the QD800 modified with a control peptide RAD. However, the behavior of QDs and other nanoparticles can vary significantly between different tumor models. The high reproducibility of QDs bioconjugated with RGD peptides and the feasibility of QD-RGDs as tumor-targeted fluorescence nanoprobe warrant the applications of QDs to molecular imaging and diagnosis in living subjects.

Activatable NIRF nanoprobe

Interdisciplinary research between scientists in the fields of molecular imaging and bionanoconjugation chemistry has generated activatable imaging nanoprobe with high-resolution imaging capabilities and ultralow background signals. Activatable imaging probe amplifies output signals in response to a specific biomolecular recognition or an environmental change in real time [77]. The unique characteristics of activatable fluorescence molecular probe could provide higher signal-to-background ratios compared to conventional “constantly active” fluorescent probe. Nanoparticle-based activatable probe has attracted significant attention because they could offer considerable advantages for obtaining optical images through their NIRF quenching properties. The design of activatable nanoprobe relies on specific tumor-related enzymes, such as cathepsin D and matrix metalloproteinases-2 (MMP-2) [78–80].

There are mainly two kinds of nanoparticle-based activatable probe. One involves energy transfer between NIRF dyes and nanoparticles with quenching properties. The polymer-based nanoparticles and Au nanoparticles are the most widely-applied quenching moieties [81]. For example, Lee and colleagues engineered 20-nm Au nanoparticles stabilized by a Cy5.5-labeled peptide substrate, Gly-Pro-Leu-Gly-Val-Arg-Gly-Cys, where the core of the peptide substrate is selectively cleaved by MMP-2. The stabilized nanoprobe has strong quenching properties with minimal background signals. Only in the presence of MMPs *in vitro* or *in vivo* when the quenching nanoparticle and the fluorescent dye are separated by cleavage of the peptide do the NIRF nanoprobe recover fluorescence [80].

The other kinds of nanoparticle-based activatable probe involve energy transfer between QDs and Au nanoparticles, where QDs serve as donors and Au nanoparticles act as quenchers. The luminescence of the QDs could be reduced by more than 70% when they were attached to the Au nanoparticles [80]. A conjugated QD-peptide-Au complex was prepared using a peptide that is a substrate for collagenase. Upon exposure to collagenase, the peptide is digested, releasing the QDs from the Au complex. The quenched (dark) nanoprobe complex is activated and the luminescence of the QDs is recovered [82]. Although many hurdles need to be overcome before QD-peptide-Au conjugates can be applied as activatable NIRF nanoprobe in living subjects, the potential advantages of this smart class of NIRF nanoprobe should inspire more research in the NIRF field.

Multimodality imaging

The combination of multiple imaging modalities can yield complementary information and offers synergistic advantages over any single modality. Compared to other imaging agents, nanoparticles have the advantages of multifunctionality and enormous flexibility, allowing

for the integration of multimodality reporting moieties, targeting ligands and even therapeutic components into one entity. The development of multifunctional nanomaterials with distinct properties makes it possible to accomplish multimodal imaging [83–85]. The future of cancer molecular imaging will increasingly rely upon multimodality, and nanoplateform-based imaging will be one of most important approaches in multimodality imaging. The combination of NIRF imaging with nuclear imaging techniques such as PET and SPECT, or anatomical imaging modalities such as MRI and CT (computed tomography), could provide more accurate physiological and spatial information, which is imperative for early cancer detection and cancer management.

The combination of NIRF nanoprobe with MRI is a major research effort. Examples include the combination of NIRF nanoprobe with superparamagnetic iron oxide or gadolinium MR contrast materials [86–88]. In addition to MRI, radionuclide imaging can also be combined with NIRF imaging, allowing increased depth penetration and absolute quantification. Recently, Cai and colleagues described the quantitative tumor targeting efficacy of dual-functional QD-based probes using both PET and NIRF imaging [89,90]. Dual-modality PET/NIRF imaging probes offer synergistic advantages over the single modality probes by overcoming the low quantitative analysis of fluorescence intensity *in vivo* and *ex vivo*. Nahrendorf and colleagues demonstrated the exquisite congruence between optical fluorescence-mediated tomography (FMT; see Glossary) and PET measurements using targeted multimodal nanoprobe [91]. Using biocompatible nanoparticles as a generic platform, the combination of radionuclides, NIR fluorochromes and targeting ligands result in multimodal nanoprobe (Figure 4). A high correlation can be seen between FMT and PET in nanoprobe concentration and spatial signal distribution both *in vitro* and in living subjects (Figure 4), which justifies the development of next generation of PET/optical molecular imaging nanoprobe.

Moreover, noninvasive PET imaging using radiolabeled nanoprobe can provide a robust and reliable measure of the biodistribution of nanoprobe in living subjects [92,93]. Although the stability and physicochemical properties of nanoprobe after radionuclide labeling should be carefully examined, the accurate evaluation of *in vivo* distribution and tumor targeting efficacy using these dual-modality probes could significantly facilitate applications of NIRF nanoprobe in biomedical research and in the clinic.

Pharmacokinetics and toxicity of NIRF nanoprobe

Comprehensive insights on how NIRF nanoprobe enter, distribute and leave living subjects are vital towards designing NIRF nanoprobe suitable for molecular imaging. In order to have a critical level of NIRF nanoprobe entering the tumor site, they must avoid uptake by both RES and MPS; however, many systemically injected NIRF nanoprobe can be rapidly cleared from the bloodstream by RES and MPS uptake, leading to the accumulation and retention in the liver and spleen. Therefore, the development of NIRF nanoprobe that evade rapid blood clearance is a key step in improving their performance as imaging agents. Indeed, surface coating, size and surface charge are three key features that influence the behavior of NIRF nanoprobe in living subjects and could guide the design of future NIRF nanoprobe for cancer molecular imaging.

Surface modification of NIRF nanoprobe with hydrophilic polymers such as PEG can enhance solubility, minimize nonspecific binding, prolong circulation time and enhance tumor specific targeting [94], but the size of the resulting nanoparticles can increase significantly. Most of the NIRF nanoprobe that have been used for imaging *in vivo* are relatively large (>20 nm in HD) and typically accumulate in the liver. Smaller nanoprobe can be cleared by the renal system, which is preferred clinically because the nanoprobe will

be less likely to be sequestered in the body for an extended period of time. QDs with neutral charge and an HD of about 5.5 nm might be cleared completely by the kidneys in a reasonable amount of time [67]. Although small nanoprobe might display short half-lives, this usually results in low accumulation in tumors [12]. NIRF nanoprobe of reasonable size should exhibit two features: the ability to extravasate and a long enough half-life to accommodate extravasation. Nonspecific binding to serum proteins in the blood, which can be influenced by the surface coating and surface charge of nanoprobe, often results in high RES uptake of nanoparticles. Thus, the three characteristics of NIRF nanoparticles size, surface coating and surface charge can mutually interfere with nanoprobe behavior in living subjects. Significant efforts are underway to investigate and optimize these parameters for improved imaging efficacy [95].

Understanding and solving the potential *in vivo* toxicity of nanoprobe is critical for their eventual clinical use [96]. Toxicity could result from NIRF nanoprobe themselves or the individual components of the nanoprobe that are released during degradation *in vivo*. To mitigate the potential toxicity, several strategies have been applied to construct biocompatible and biodegradable nanoprobe composed of low toxicity building blocks. CPNPs encapsulated clinically approved ICG fluorophores are biocompatible and biodegradable [20]. Biodegradable NIR silicon nanoparticles with no detectable toxicity to small animals have also been reported [43]. Dye-containing water-soluble polymers might have a chance for clinical use because the polymers can be designed to be biocompatible and degradable [25,26].

Although Cd-based QDs showed cytotoxicity under extreme conditions, most toxicology data are derived from *in vitro* studies and might not reflect *in vivo* responses. *In vivo* responses are the ultimate concern for the clinical translation of nanoprobe. Hauck and colleagues [95] described systematic toxicity of Cd-based QDs using healthy rats as a model. The QD formulations (CdSe/ZnS core/shell QDs with polymer, PEG or BSA coating) do not cause appreciable toxicity even after they breakdown in rats over time [97]. Similarly, systematic evaluation of SWNT toxicity in animals revealed no evidence of toxicity for over four months after intravenous injection [98]. Although these data are preliminary and need confirmation, in aggregate they are encouraging and thereby compel us to research further the use of these nanoparticles for nanoprobe development.

Challenges and perspectives

Recent and rapid development of synthesis technologies for nanomaterials has created enormous opportunities for the design of specific and sensitive NIRF nanoprobe for cancer molecular imaging. The potential to diagnose and monitor altered physiological changes of cancer in patients by using NIRF nanoprobe is coming closer to reality. However, there remain considerable challenges pertaining to applications of NIRF nanoprobe in humans. In addition to the purity, dispensability and stability of NIRF nanoprobe in physiological environments, the variable physicochemical properties of different NIRF nanoprobe might produce unexpected outcomes *in vivo*. Several studies have shown that NIRF nanoprobe might be systemically distributed in organs and tissues. Absorption, distribution, metabolism and excretion characteristics are highly variable for NIRF nanoprobe because of the wide variation in the physicochemical properties of nanomaterials [95,99,100].

Progress toward the clinical adaptation of NIRF nanoprobe-based molecular imaging might be slow as probe for clinical use generally undergo stringent iterative redesign, optimization and validation that can take many years. Many issues need to be overcome before the NIRF nanoprobe will be ready for clinical translation (Box 1). The pharmacokinetics and toxicity of the NIRF nanoprobe should be investigated in parallel

with their imaging potential. Food and Drug Administration (FDA) approved, biodegradable and biocompatible materials might be good starting materials for constructing the NIRF nanoprobes. Although there are examples for successful imaging of tumors in small animal models using NIRF nanoprobes, an unfavorable biodistribution such as highly nonspecific accumulation in the RES still needs to be resolved. The major challenge is to develop the surface coating nanomaterials that can help NIRF nanoprobes escape from the RES and also provide active functional groups for controllable bioconjugation of specific targeting molecules. For NIRF imaging of deep tissues, further innovations in probe preparation are necessary to generate NIRF nanoprobes with high quantum yield and deep tissue penetration. In the clinical setting, optical imaging is relevant for tissues close to the surface of skin, tissues accessible by endoscopy and intraoperative visualization. The use of multifunctional nanoparticles (e.g. paramagnetic NIRF nanoprobes) would have great advantages for providing tumor assessment and intraoperative surgical guidance for tumor tissue resection [101,102], because the combination of NIRF imaging with MRI, PET and X-ray are expected to provide anatomical and biological information with accurate location and quantification of the fluorescence signal.

In summary, the successful development of NIRF nanoprobes and their potential applications in cancer molecular imaging have inspired increasing research interests in nanomedicine and nanobiotechnology. The applications of NIRF nanoprobes in medical research have already been significant. Although the practical clinical application of NIRF nanoprobes has proved challenging, continued collaborations among the fields of materials science, chemistry, molecular biology and imaging, preclinical and clinical medicine, and the regulatory authorities will no doubt speed up the translational process so eventually the impact of nanomedicine in the diagnosis and management of cancer can be realized.

Box 1. Aspects of nanoprobes that need to be addressed before clinical translation will be possible

- Biodegradable and biocompatible materials should be considered as starting materials for constructing the NIRF nanoprobes
- Synthesis of novel NIRF nanoprobes with high quantum yield and deep tissue penetration
- Sufficient photostability for applications in living subjects
- Appropriate surface coating for decreasing nonspecific binding while in circulation or during RES uptake
- A reasonable size of NIRF nanoprobes to allow extravasation and a half-life long enough for extravasation to occur
- Development of targeted NIRF nanoprobes with high specificity and selectivity

Glossary

Raman signatures	the Raman spectrum of a particular material shows the “fingerprints”, which are known as spectra signatures and enable identification of the materials that make up a scanned object
Fermi wavelength	the size scale is related to $E_{\text{Fermi}}/N^{1/3}$, predicted by the free-electron model of metallic behavior (about 0.5 nm for gold and silver). E_{Fermi}

Fluorescence-mediated tomography (FMT)

(Fermi energy) is the energy of the highest occupied quantum state in a system of fermions at absolute zero temperature

a method of molecular imaging shows the distribution of a NIRF probes in the region of an animal by three-dimensional tomographic images

Acknowledgments

This work was partially supported by NCI/NIH R21 CA121842 (to Z.C.), NCI In vivo Cellular & Molecular Imaging Centers (ICMIC) P50 (to S.S.G.) and NCI Center for Cancer Nanotechnology Excellence Grant U54 CA119367 (to S.S.G.).

References

1. Massoud TF, Gambhir SS. Molecular imaging in living subjects: seeing fundamental biological processes in a new light. *Genes Dev* 2003;17:545–580. [PubMed: 12629038]
2. Weissleder R. Molecular imaging in cancer. *Science* 2006;312:1168–1171. [PubMed: 16728630]
3. Quon A, Gambhir SS. FDG-PET and beyond: molecular breast cancer imaging. *J. Clin. Oncol* 2005;23:1664–1673. [PubMed: 15755974]
4. Weissleder R, Pittet MJ. Imaging in the era of molecular oncology. *Nature* 2008;452:580–589. [PubMed: 18385732]
5. Willmann JK, et al. Molecular imaging in drug development. *Nat. Rev. Drug Discov* 2008;7:591–607. [PubMed: 18591980]
6. Cai WB, et al. PET of vascular endothelial growth factor receptor expression. *J. Nucl. Med* 2006;47:2048–2056. [PubMed: 17138749]
7. Holman BL, Devous MD. Functional brain SPECT - the emergence of a powerful clinical method. *J. Nucl. Med* 1992;33:1888–1904. [PubMed: 1403163]
8. Harisinghani MG, et al. Noninvasive detection of clinically occult lymph-node metastases in prostate cancer. *N. Engl. J. Med* 2003;348 2491-U5.
9. McCarthy JR, Weissleder R. Multifunctional magnetic nanoparticles for targeted imaging and therapy. *Adv. Drug Deliv. Rev* 2008;60:1241–1251. [PubMed: 18508157]
10. Gao JH, et al. Multifunctional magnetic nanoparticles: design, synthesis, and biomedical applications. *Acc. Chem. Res* 2009;42:1097–1107. [PubMed: 19476332]
11. Ballou B, et al. Fluorescence imaging of tumors *in vivo*. *Curr. Med. Chem* 2005;12:795–805. [PubMed: 15853712]
12. Hilderbrand SA, Weissleder R. Near-infrared fluorescence: application to *in vivo* molecular imaging. *Curr. Opin. Chem. Biol* 2010;14:71–79. [PubMed: 19879798]
13. Gao JH, et al. Near-infrared quantum dots as optical probes for tumor imaging. *Curr. Top. Med. Chem* 2010;10:1147–1157. [PubMed: 20388111]
14. Minchin RF, Martin DJ. Nanoparticles for molecular imaging--an overview. *Endocrinology* 2010;151:474–481. [PubMed: 20016027]
15. Yang X, et al. Nanoparticles for photoacoustic imaging. *Wiley Interdiscip. Rev. Nanomed. Nanobiotechnol* 2009;1:360–368. [PubMed: 20049803]
16. De la Zerda A, et al. Carbon nanotubes as photoacoustic molecular imaging agents in living mice. *Nat. Nanotechnol* 2008;3:557–562. [PubMed: 18772918]
17. Lee JH, et al. Artificially engineered magnetic nanoparticles for ultra-sensitive molecular imaging. *Nat. Med* 2007;13:95–99. [PubMed: 17187073]
18. He XX, et al. *In vivo* near-infrared fluorescence imaging of cancer with nanoparticles-based probes. *Wiley Interdiscip. Rev. Nanomed. Nanobiotechnol* 2010;2:349–366. [PubMed: 20564463]
19. Vetrone F, Capobianco JA. Lanthanide-doped fluoride nanoparticles: luminescence, upconversion, and biological applications. *Int. J. Nanotechnol* 2008;5:1306–1339.

20. Altinoglu EI, et al. Near-infrared emitting fluorophore-doped calcium phosphate nanoparticles for *in vivo* imaging of human breast cancer. *ACS Nano* 2008;2:2075–2084. [PubMed: 19206454]
21. Lee CH, et al. Near-infrared mesoporous silica nanoparticles for optical imaging: characterization and *in vivo* biodistribution. *Adv. Funct. Mater* 2009;19:215–222.
22. Tanisaka H, et al. Near-infrared fluorescent labeled peptosome for application to cancer imaging. *Bioconjugate Chem* 2008;19:109–117.
23. Cao WG, et al. Synthesis and evaluation of a stable bacteriochlorophyll-analog and its incorporation into high-density lipoprotein nanoparticles for tumor imaging. *Bioconjugate Chem* 2009;20:2023–2031.
24. Mulder WJM, et al. Nanoparticulate assemblies of amphiphiles and diagnostically active materials for multimodality imaging. *Accounts Chem. Res* 2009;42:904–914.
25. Yang Z, et al. Long-circulating near-infrared fluorescence core-cross-linked polymeric micelles: Synthesis, characterization, and dual nuclear/optical imaging. *Biomacromolecules* 2007;8:3422–3428. [PubMed: 17958440]
26. Yang Z, et al. Pharmacokinetics and biodistribution of near-infrared fluorescence polymeric nanoparticles. *Nanotechnology* 2009;20:165101. [PubMed: 19420561]
27. Bruchez M, et al. Semiconductor nanocrystals as fluorescent biological labels. *Science* 1998;281:2013–2016. [PubMed: 9748157]
28. Chan WCW, Nie SM. Quantum dot bioconjugates for ultrasensitive nonisotopic detection. *Science* 1998;281:2016–2018. [PubMed: 9748158]
29. Michalet X, et al. Quantum dots for live cells, *in vivo* imaging, and diagnostics. *Science* 2005;307:538–544. [PubMed: 15681376]
30. Medintz IL, et al. Self-assembled nanoscale biosensors based on quantum dot FRET donors. *Nat. Mater* 2003;2:630–638. [PubMed: 12942071]
31. Gill R, et al. Semiconductor quantum dots for bioanalysis. *Angew. Chem., Int. Edit* 2008;47:7602–7625.
32. Smith AM, et al. Bioconjugated quantum dots for *in vivo* molecular and cellular imaging. *Adv. Drug Deliv. Rev* 2008;60:1226–1240. [PubMed: 18495291]
33. Frangioni JV. *In vivo* near-infrared fluorescence imaging. *Curr. Opin. Chem. Biol* 2003;7:626–634. [PubMed: 14580568]
34. Tsay JM, et al. Hybrid approach to the synthesis of highly luminescent CdTe/ZnS and CdHgTe/ZnS nanocrystals. *J. Am. Chem. Soc* 2004;126:1926–1927. [PubMed: 14971912]
35. Kim S, et al. Near-infrared fluorescent type II quantum dots for sentinel lymph node mapping. *Nat. Biotechnol* 2004;22:93–97. [PubMed: 14661026]
36. Kim SW, et al. Engineering InAs_xP_{1-x}/InP/ZnSe III-V alloyed core/shell quantum dots for the near-infrared. *J. Am. Chem. Soc* 2005;127:10526–10532. [PubMed: 16045339]
37. Allen PM, Bawendi MG. Ternary I-III-VI quantum dots luminescent in the red to near-infrared. *J. Am. Chem. Soc* 2008;130:9240–9241. [PubMed: 18582061]
38. Xie RG, Peng XG. Synthesis of Cu-doped InP nanocrystals (d-dots) with ZnSe diffusion barrier as efficient and color-tunable NIR emitters. *J. Am. Chem. Soc* 2009;131:10645–10651. [PubMed: 19588970]
39. Derfus AM, et al. Probing the cytotoxicity of semiconductor quantum dots. *Nano Lett* 2004;4:11–18.
40. Kirchner C, et al. Cytotoxicity of colloidal CdSe and CdSe/ZnS nanoparticles. *Nano Lett* 2005;5:331–338. [PubMed: 15794621]
41. Xie RG, et al. Formation of high-quality I-III-VI semiconductor nanocrystals by tuning relative reactivity of cationic precursors. *J. Am. Chem. Soc* 2009;131:5691–5697. [PubMed: 19331353]
42. Sun YP, et al. Quantum-sized carbon dots for bright and colorful photoluminescence. *J. Am. Chem. Soc* 2006;128:7756–7757. [PubMed: 16771487]
43. Park JH, et al. Biodegradable luminescent porous silicon nanoparticles for *in vivo* applications. *Nat. Mater* 2009;8:331–336. [PubMed: 19234444]
44. Burns AA, et al. Fluorescent silica nanoparticles with efficient urinary excretion for nanomedicine. *Nano Lett* 2009;9:442–448. [PubMed: 19099455]

45. De A, Gambhir SS. Noninvasive imaging of protein-protein interactions from live cells and living subjects using bioluminescence resonance energy transfer. *FASEB J* 2005;19:2017. [PubMed: 16204354]
46. De A, et al. BRET3: a red-shifted bioluminescence resonance energy transfer (BRET)-based integrated platform for imaging protein-protein interactions from single live cells and living animals. *FASEB J* 2009;23:2702–2709. [PubMed: 19351700]
47. So MK, et al. Self-illuminating quantum dot conjugates for *in vivo* imaging. *Nat. Biotech* 2006;24:339–343.
48. Zhang Y, et al. HaloTag protein-mediated site-specific conjugation of bioluminescent proteins to quantum dots. *Angew. Chem., Int. Ed* 2006;45:4936–4940.
49. Xia ZY, Rao JH. Biosensing and imaging based on bioluminescence resonance energy transfer. *Curr. Opin. Biotechnol* 2009;20:37–44. [PubMed: 19216068]
50. Loening AM, et al. Red-shifted Renilla reniformis luciferase variants for imaging in living subjects. *Nat. Methods* 2007;4:641–643. [PubMed: 17618292]
51. Liu HG, et al. Radiation-luminescence-excited quantum dots for *in vivo* multiplexed optical imaging. *Small* 2010;6:1087–1091. [PubMed: 20473988]
52. O'Connell MJ, et al. Band gap fluorescence from individual single-walled carbon nanotubes. *Science* 2002;297:593–596. [PubMed: 12142535]
53. Amiot CL, et al. Near-infrared fluorescent materials for sensing of biological targets. *Sensors* 2008;8:3082–3105.
54. Hong H, et al. Molecular imaging with single-walled carbon nanotubes. *Nano Today* 2009;4:252–261.
55. Liu Z, et al. Carbon nanotubes in biology and medicine: *in vitro* and *in vivo* detection, imaging and drug delivery. *Nano Res* 2009;2:85–120. [PubMed: 20174481]
56. Huang CC, et al. Bioconjugated gold nanodots and nanoparticles for protein assays based on photoluminescence quenching. *Anal. Chem* 2008;80:1497–1504. [PubMed: 18237154]
57. Qian XM, et al. Surface-enhanced raman nanoparticle beacons based on bioconjugated gold nanocrystals and long range plasmonic coupling. *J. Am. Chem. Soc* 2008;130:14934–14935. [PubMed: 18937463]
58. Niidome T, et al. *In vivo* monitoring of intravenously injected gold nanorods using near-infrared light. *Small* 2008;4:1001–1007. [PubMed: 18581412]
59. Keren S, et al. Noninvasive molecular imaging of small living subjects using Raman spectroscopy. *Proc. Natl. Acad. Sci. USA* 2008;105:5844–5849. [PubMed: 18378895]
60. Zheng J, et al. Highly fluorescent noble-metal quantum dots. *Annu. Rev. Phys. Chem* 2007;58:409–431. [PubMed: 17105412]
61. Zheng J, et al. High quantum yield blue emission from water-soluble Au-8 nanodots. *J. Am. Chem. Soc* 2003;125:7780–7781. [PubMed: 12822978]
62. Bao YP, et al. Nanoparticle-free synthesis of fluorescent gold nanoclusters at physiological temperature. *J. Phys. Chem. C* 2007;111:12194–12198.
63. Huang CC, et al. Synthesis of wavelength-tunable luminescent gold and gold/silver nanodots. *J. Mater. Chem* 2009;19:755–759.
64. Xie JP, et al. Protein-directed synthesis of highly fluorescent gold nanoclusters. *J. Am. Chem. Soc* 2009;131:888–889. [PubMed: 19123810]
65. Dass CR. Tumour angiogenesis, vascular biology and enhanced drug delivery. *J. Drug Target* 2004;12:245–255. [PubMed: 15512775]
66. Davis ME, et al. Nanoparticle therapeutics: an emerging treatment modality for cancer. *Nat. Rev. Drug Discov* 2008;7:771–782. [PubMed: 18758474]
67. Choi HS, et al. Renal clearance of quantum dots. *Nat. Biotechnol* 2007;25:1165–1170. [PubMed: 17891134]
68. Choi HS, et al. Design considerations for tumour-targeted nanoparticles. *Nat. Nanotechnol* 2010;5:42–47. [PubMed: 19893516]
69. Gao JH, et al. Ultrasmall near-infrared non-cadmium quantum dots for *in vivo* tumor imaging. *Small* 2010;6:256–261. [PubMed: 19911392]

70. Hama Y, et al. Simultaneous two-color spectral fluorescence lymphangiography with near infrared quantum dots to map two lymphatic flows from the breast and the upper extremity. *Breast Cancer Res. Treat* 2007;103:23–28. [PubMed: 17028977]
71. Welscher K, et al. A route to brightly fluorescent carbon nanotubes for near-infrared imaging in mice. *Nat. Nanotechnol* 2009;4:773–780. [PubMed: 19893526]
72. Gao XH, et al. *In vivo* cancer targeting and imaging with semiconductor quantum dots. *Nat. Biotechnol* 2004;22:969–976. [PubMed: 15258594]
73. Cai WB, et al. Peptide-labeled near-infrared quantum dots for imaging tumor vasculature in living subjects. *Nano Lett* 2006;6:669–676. [PubMed: 16608262]
74. Cai WB, Chen XY. Preparation of peptide-conjugated quantum dots for tumor vasculature-targeted imaging. *Nat. Protoc* 2008;3:89–96. [PubMed: 18193025]
75. Gao JH, et al. *In vivo* tumor-targeted fluorescence imaging using near-infrared non-cadmium quantum dots. *Bioconjugate Chem* 2010;21:604–609.
76. Smith BR, et al. Real-time intravital imaging of RGD-quantum dot binding to luminal endothelium in mouse tumor neovasculature. *Nano Lett* 2008;8:2599–2606. [PubMed: 18386933]
77. Schellenberger E. Bioresponsive nanosensors in medical imaging. *J. R. Soc. Interface* 2010;7:S83–S91. [PubMed: 19846442]
78. Jiang T, et al. Tumor imaging by means of proteolytic activation of cell-penetrating peptides. *Proc. Natl. Acad. Sci. USA* 2004;101:17867–17872. [PubMed: 15601762]
79. Lee S, et al. Activatable imaging probes with amplified fluorescent signals. *Chem. Commun* 2008:4250–4260.
80. Lee S, et al. A near-infrared-fluorescence-quenched gold-nanoparticle imaging probe for *in vivo* drug screening and protease activity determination. *Angew. Chem., Int. Edit* 2008;47:2804–2807.
81. Lee S, et al. Activatable Molecular Probes for Cancer Imaging. *Curr. Top. Med. Chem* 2010;10:1135–1144. [PubMed: 20388112]
82. Chang E, et al. Protease-activated quantum dot probes. *Biochem. Biophys. Res. Commun* 2005;334:1317–1321. [PubMed: 16039606]
83. Cai WB, Chen XY. Nanoplatforams for targeted molecular imaging in living subjects. *Small* 2007;3:1840–1854. [PubMed: 17943716]
84. Mulder WJM, et al. Magnetic and fluorescent nanoparticles for multimodality imaging. *Nanomedicine* 2007;2:307–324. [PubMed: 17716176]
85. Cai WB, Chen XY. Multimodality molecular imaging of tumor angiogenesis. *J. Nucl. Med* 2008;49:113S–128S. [PubMed: 18523069]
86. Josephson L, et al. Near-infrared fluorescent nanoparticles as combined MR/optical imaging probes. *Bioconjugate Chem* 2002;13:554–560.
87. Ostendorp M, et al. Quantitative molecular magnetic resonance imaging of tumor angiogenesis using cNGR-labeled paramagnetic quantum dots. *Cancer Res* 2008;68:7676–7683. [PubMed: 18794157]
88. Park JH, et al. Micellar hybrid nanoparticles for simultaneous magnetofluorescent imaging and drug delivery. *Angew. Chem., Int. Ed* 2008;47:7284–7288.
89. Cai WB, et al. Dual-function probe for PET and near-infrared fluorescence imaging of tumor vasculature. *J. Nucl. Med* 2007;48:1862–1870. [PubMed: 17942800]
90. Chen K, et al. Dual-modality optical and positron emission tomography imaging of vascular endothelial growth factor receptor on tumor vasculature using quantum dots. *Eur. J. Nucl. Med. Mol. Imaging* 2008;35:2235–2244. [PubMed: 18566815]
91. Nahrendorf M, et al. Hybrid PET-optical imaging using targeted probes. *Proc. Natl. Acad. Sci. USA* 2010;107:7910–7915. [PubMed: 20385821]
92. Schipper ML, et al. MicroPET-based biodistribution of quantum dots in living mice. *J. Nucl. Med* 2007;48:1511–1518. [PubMed: 17704240]
93. Schipper ML, et al. Particle size, surface coating, and PEGylation influence the biodistribution of quantum dots in living mice. *Small* 2009;5:126–134. [PubMed: 19051182]
94. Storm G, et al. Surface modification of nanoparticles to oppose uptake by the mononuclear phagocyte system. *Adv. Drug Deliv. Rev* 1995;17:31–48.

95. Aillon KL, et al. Effects of nanomaterial physicochemical properties on *in vivo* toxicity. *Adv. Drug Deliv. Rev* 2009;61:457–466. [PubMed: 19386275]
96. Lewinski N, et al. Cytotoxicity of nanoparticles. *Small* 2008;4:26–49. [PubMed: 18165959]
97. Hauck TS, et al. *In vivo* quantum-dot toxicity assessment. *Small* 2010;6:138–144. [PubMed: 19743433]
98. Schipper ML, et al. A pilot toxicology study of single-walled carbon nanotubes in a small sample of mice. *Nat. Nanotechnol* 2008;3:216–221. [PubMed: 18654506]
99. Hardman R. A toxicologic review of quantum dots: Toxicity depends on physicochemical and environmental factors. *Environ. Health Perspect* 2006;114:165–172. [PubMed: 16451849]
100. Nel A, et al. Toxic potential of materials at the nanolevel. *Science* 2006;311:622–627. [PubMed: 16456071]
101. Nguyen QT, et al. Surgery with molecular fluorescence imaging using activatable cell-penetrating peptides decreases residual cancer and improves survival. *Proc. Natl. Acad. Sci. USA* 2010;107:4317–4322. [PubMed: 20160097]
102. Olson ES, et al. Activatable cell penetrating peptides linked to nanoparticles as dual probes for *in vivo* fluorescence and MR imaging of proteases. *Proc. Natl. Acad. Sci. USA* 2010;107:4311–4316. [PubMed: 20160077]

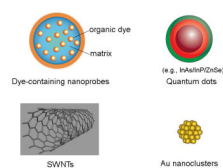


Figure 1.
Representative nanomaterial-based NIRF nanoprobe for molecular imaging in living subjects.

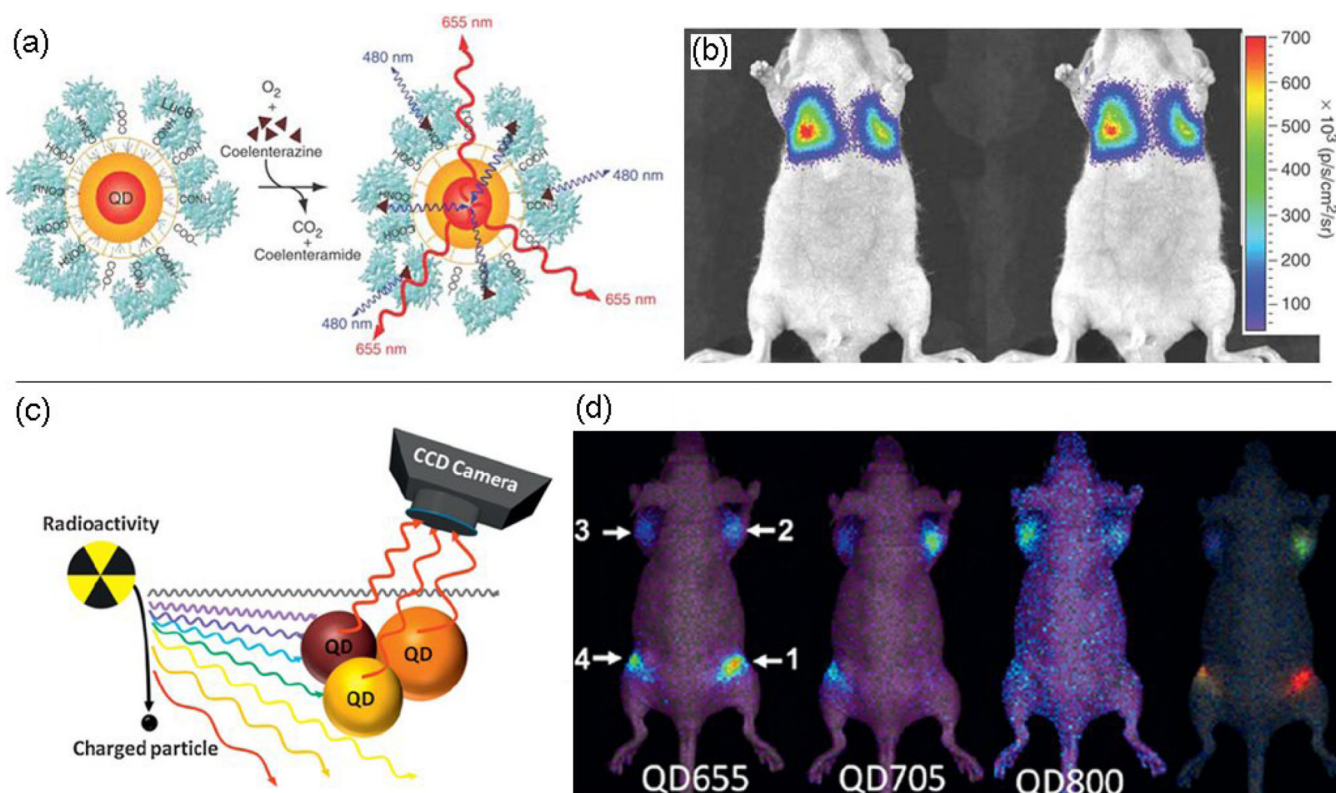


Figure 2.

Self-illuminating nanoprobe based on NIRF QDs. (a) Molecular imaging of bioluminescent QD conjugates in small animals based on BRET. The scheme shows a QD that is covalently coupled to a BRET donor, Luc8. (b) Representative bioluminescence images of a nude mouse injected via tail vein with labeled cells, acquired with a filter (575–650 nm) (left) and without any filter (right). Reprinted with permission from Ref. [47]. Copyright 2006, Nature Publishing Group. (c) The scheme shows the radiation-luminescence-excited QDs for optical imaging. (d) Multiplexed *in vivo* radioactivity illuminated QD imaging shows the spectral imaging of the QD655, QD705 and QD800 in mice, respectively, and the spectral unmixed image of the same mouse (right). Reprinted with permission from Ref. [51]. Copyright 2010, Wiley-VCH.

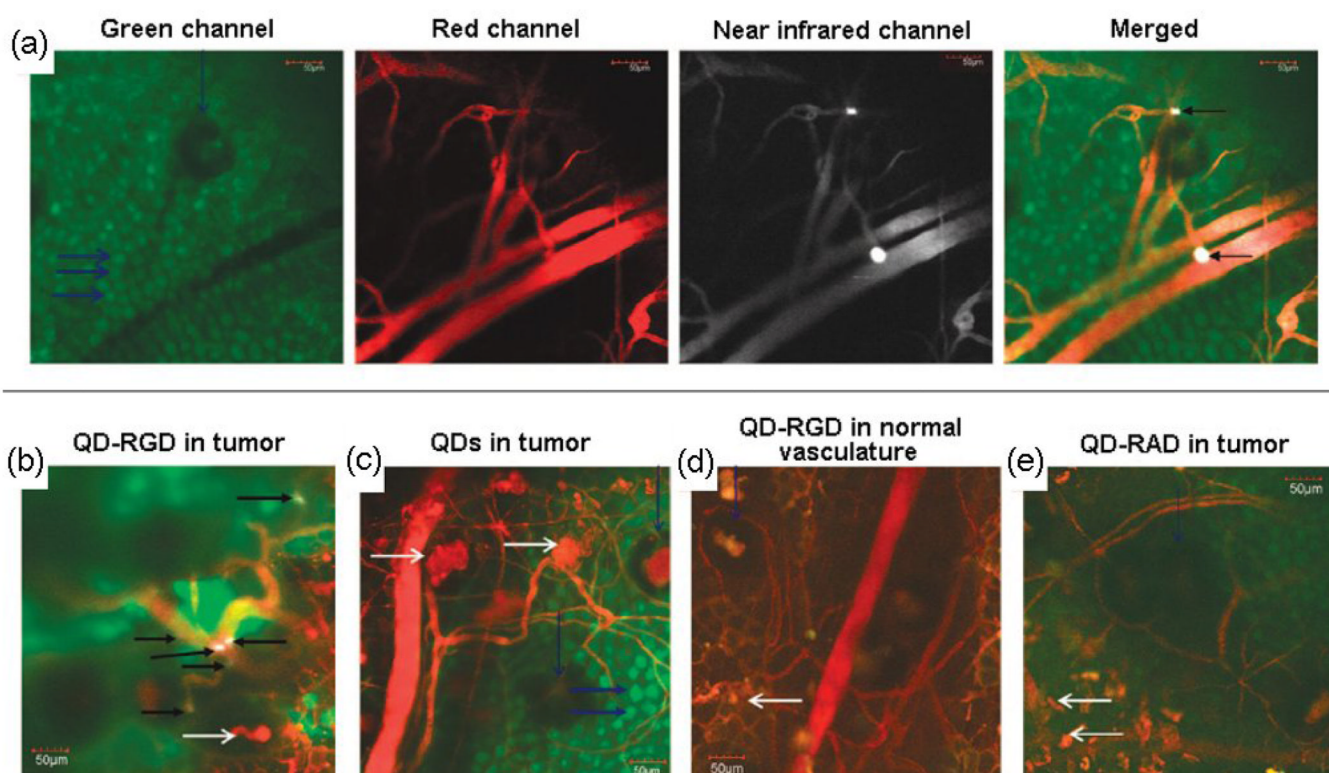


Figure 3.

Direct visualization of QD800-RGD binding to tumor vessel endothelium and controls in a living mouse ear tumor model using intravital microscopy. (a) Each panel displays different output channels of the identical imaging plane along the row. In the green channel, individual enhanced green fluorescent protein (EGFP)-expressing cancer cells are visible, while the red channel shows the tumor's vasculature via injection of Angiosense dye. The NIR channel shows intravascularly administered QDs that remain in the vessels. Binding events are visible by a bright white signal. These are demarcated by arrows in the rightmost merged image in which all three channels have been overlaid. (b) Merged image of a different mouse using QD800-RGD. Individual cells are not generally visible. (c–e) Typical images without binding in each control condition: (c) Tumor neovasculature containing unconjugated QDs, (d) normal vasculature containing QD800-RGD, and (e) tumor neovasculature containing QD800-RAD. Reprinted with permission from Ref. [76]. Copyright 2008, American Chemical Society.

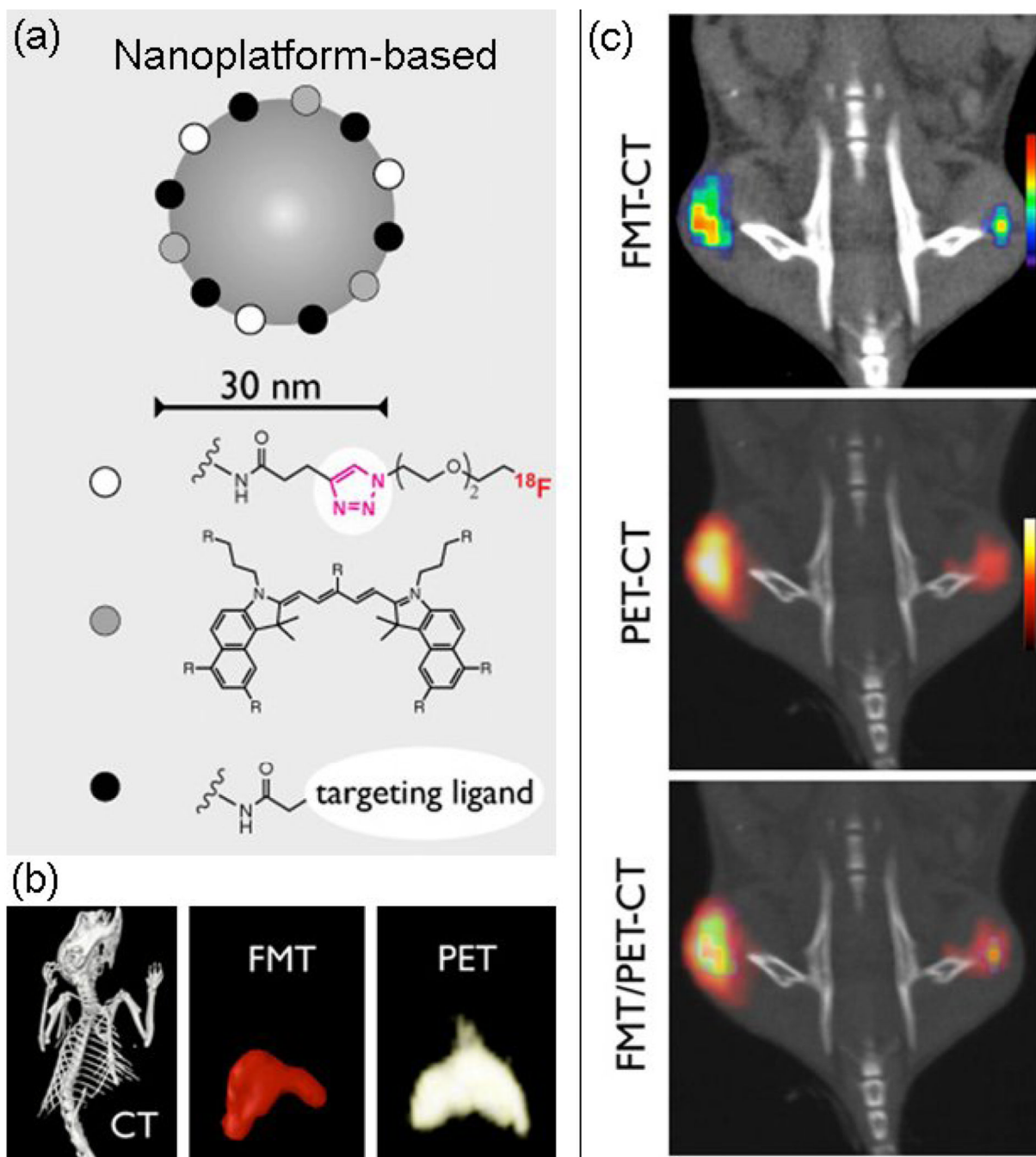


Figure 4.

Hybrid FMT/PET-CT imaging using multimodal NIRF nanoprobes. (a) The scheme shows nanoplateform-based (Dextran-coated iron oxide nanoparticles, CLIO) nanoprobes containing radionuclides, NIR fluorochromes (e.g. VT680) and affinity ligands, such as peptides and small molecules. (b) The three-dimensional reconstruction of CT, FMT and PET dataset after injection of ^{18}F fluorine-CLIO-VT680 into a control mouse. Signals are predominantly seen in the liver and spleen. (c) Comparison of FMT-CT, PET-CT and FMT/PET-CT reconstructions in a representative mouse with bilateral flank tumors showing correlation of spatial distribution and the amplitude of signals. Reprinted with permission from Ref. [91]. Copyright 2010, the National Academy of Sciences.